Available online at www.sciencedirect.com
ScienceDirect
Bioorganic & Medicinal Chemistry Letters 18 (2008) 2825–2829
Bioorganic & Medicinal Chemistry Letters

Dual binding site inhibitors of B-RAF kinase

Ronald L. Wolin,* Scott D. Bembenek, Jianmei Wei, Shelby Crawford, Katherine Lundeen, Anders Brunmark, Lars Karlsson, James P. Edwards and Jonathan M. Blevitt

Johnson & Johnson Pharmaceutical Research & Development, L.L.C., 3210 Merryfield Row, San Diego, CA 92121, USA

Received 6 February 2008; revised 28 March 2008; accepted 1 April 2008
Available online 4 April 2008

Abstract—Computer aided modeling guided the design of a series of diarylimidazole compounds (**11**–**22**) intended to interact with both the ATP and adjacent allosteric binding domains of B-RAF kinase. Their ability to inhibit the function of B-RAF kinase and intracellular ERK1/2 phosphorylation were evaluated.

The RAF (Ras Activating Factor) family of serine/threonine kinases are members of the MAPK kinase signaling cascade and participate in relaying extracellular signals from the cell surface to the nucleus. The RAF family comprises of three isoforms; A-RAF, B-RAF, and C-RAF, which are involved in cell growth, differentiation, and apoptosis. Clinically, it has been determined that ~66% of melanomas, ~36% of thyroid tumors, and ~10% of colon cancers in humans can be correlated with mutations that have occurred in the B-RAF kinase domain.[1] While over 40 different mutations in the kinase domain have been identified, the most prevalent mutation arises from the replacement of a valine residue with a glutamic acid residue located at position 600. This substitution, which lies within the kinase activation loop, essentially precludes the need for phosphorylation and results in constitutively active B-RAF that displays approximately a 500-fold increase in kinase activity over the wild-type isoform.[2] As a result, the activation of the MAPK signaling cascade through mutant B-RAF has been linked to tumorigenesis in several types of tumors. Based upon these observations, and the fact that B-RAF is considered an important therapeutic target for cancer management,[3] we embarked upon a chemistry effort towards identifying a small molecule that would inhibit this signaling pathway.

High-throughput-screening of our compound collection identified several diarylimidazoles as low nM inhibitors of B-RAF kinase of which **1** served as a general representation of the type of hits identified. Maintaining an ortho substituent (i.e., Cl) on the aryl ring attached at the C-4 position of the imidazole ring was important for retaining B-RAF kinase affinity and selectivity. Substituents (i.e., Cl) at the *meta*- or *para*-position of the C-4 aryl ring displayed less selectivity for B-RAF. Compound **1** was chosen as an attractive lead since related analogs suffered from poor physiochemical properties and/or microsomal instability. Via slight SAR modifications we prepared a derivative **2** that inhibited B-RAF with improved potency and possessed comparable solubility and metabolic stability parameters.[4] The 2,5-dichloro substituent was mainly responsible for the boost in kinase potency, and the conversion of the *t*-butylurea to the cyclic urea was responsible for improving the solubility profile (see Fig. 1).

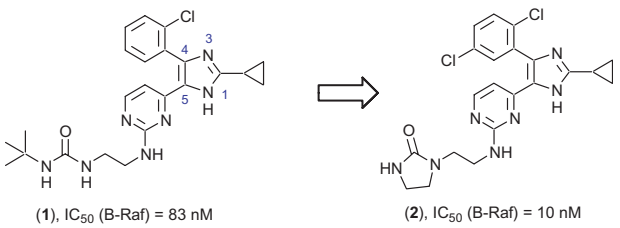

Figure 1. SAR modifications.

Keywords: B-RAF; Kinase inhibitors; Diarylimidazoles.
* Corresponding author. Tel.: +1 858 784 3133; fax: +1 858 784 3116; e-mail: RWOLIN@PRDUS.JNJ.COM

0960-894X/$ - see front matter © 2008 Elsevier Ltd. All rights reserved.
doi:10.1016/j.bmcl.2008.04.002

The report from Wan and co-workers[2] detailing the first x-ray crystal structure for a small molecule ligand (**3**, BAY-43-9006, Sorafenib)[5] bound to B-RAF kinase prompted us to compare our chemical series to the crystal structure coordinates of Sorfenib to determine what binding elements of the kinase may be shared by the two molecules. The crystallographic data revealed the pyridyl amide portion of (**3**) occupies the relatively conserved ATP pocket while the aryl urea portion (motif E, Fig. 2) of the molecule resides in an uncharacteristically deep hydrophobic pocket and serves as the allosteric binding motif. Consequently, the unique hydrophobic pocket of B-RAF appeared to offer an opportunity to achieve a less promiscuous kinase inhibitor. From our docking model studies using the coordinates deposited by Wan et. al. (PDB ID 1UWH)[2] on a series of diarylimidazoles related to **1**, it appeared that a *meta*-anilino intermediate (**8**, Scheme 1) would provide a handle for directing a branching group into the hydrophobic pocket as desired. Additionally, one could envision that the A and B rings of **2** approximate the conformation occupied by rings C and D of (**3**). The main difference effecting the spatial orientation of the aryl rings is the scaffold linking the two aryl rings together; an imidazole ring versus an ether linkage (Figs. 2 and 3).

To test the dual-site inhibitor hypothesis, we constructed a number of *meta*-substituted compounds. The synthetic route used to assemble these inhibitors is outlined in Scheme 1. The anion of pyrimidine **4** was condensed with the Weinreb amide (derived from 3-aminobenzoic acid)[6] to afford the aryl ketone **5**. Kornblum[7] oxidation of **5** provided the α-diketone **6**, which was treated with cyclopropane carboxaldehyde or trifluoroacetaldehyde hydrate in the presence of ammonium acetate and acetic acid to afford the C2-substituted imidazoles **7**. Hydrolysis of the ethyl carbamate under basic conditions afforded the amine **8**, which was subsequently treated with the appropriate electrophile to provide the urea, sulfonamide or amide intermediates. Oxidation of the thiomethyl moiety employing *m*-CPBA afforded the corresponding sulfoxide or sulfone **9** which was subsequently displaced with the requisite amine in refluxing dioxane to provide adducts **10** in yields ranging from 40% to 70%. Displacement with 3-aminobenzamide required the addition of TFA to facilitate this transformation.

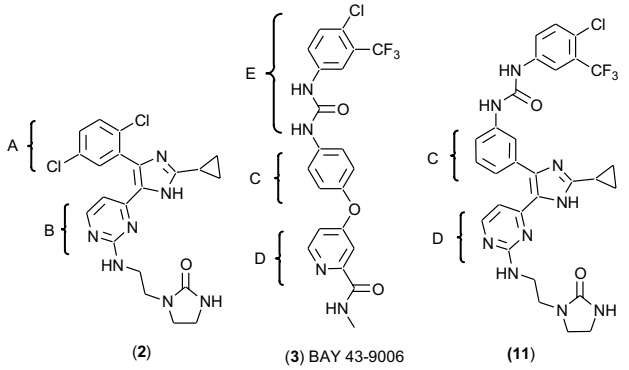

Figure 2. Rationale for the hybrid strategy.

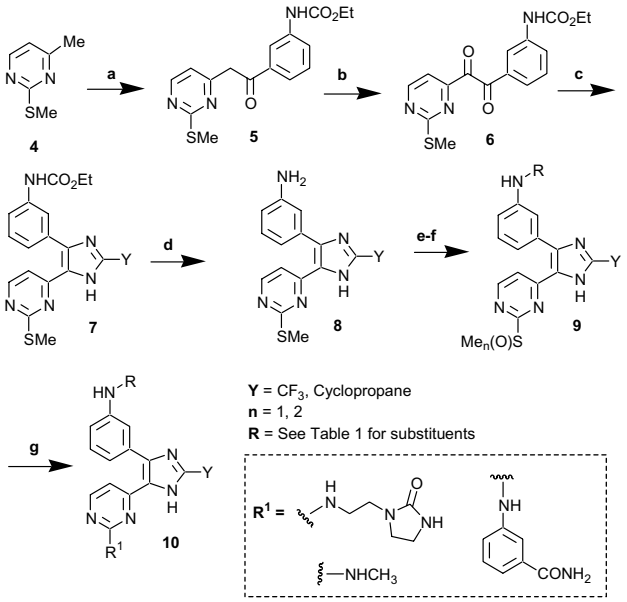

Scheme 1. Synthetic route to the diarylimidazole analogs. Reagents and conditions: (a) LiHMDS, THF, 0 °C, 30 min, then the Weinreb Amide, 0 °C → rt, 24 h (b) Br_2, CH_2Cl_2, 0 °C → rt, 1 h, then, DMSO, Et_3N, 65 °C, 1.5 h. (c) Y-CHO, NH_4OAc, HOAc, 65 °C, 16 h (d) KOH, H_2O, EtOH, 80 °C, 24 h (e) 4-chlorophenyl acetylchloride, or 3,4-dichlorophenyl sulfonylchloride, or 4-chloro-3-trifluoromethylphenyl isocyanate Et_3N, CH_2Cl_2, (f) UHP, TFAA, CH_3CN, 0 °C, 45 min, or m-CPBA, CH_2Cl_2, 0 °C, 30 min (g) R^1-NH_2, dioxane, 80–120 °C, 4–16 h.

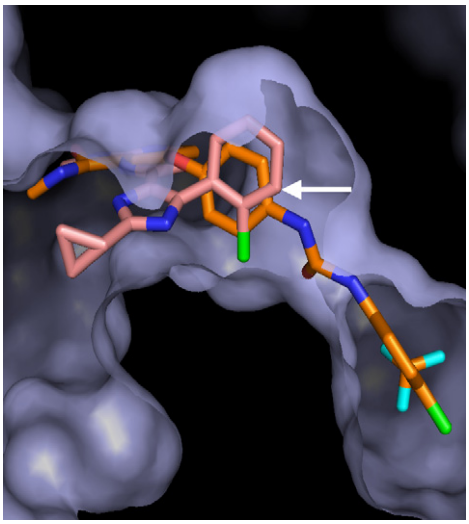

Figure 3. Crystal structure of Sorafenib overlaid with the docking model of our desired template in B-RAF. The arrow emphasizes the predicted position (meta) for attaching substituents to our template to allow for access to the hydrophobic pocket.

For consistency, the same urea component present in Sorafenib (**3**) was installed onto the aniline intermediate **10** and three different groups were appended to the pyrimidine ring for evaluation (R^1 = methylamine, 3-aminobenzamide, and 1-(2-amino-ethyl)-imidazolidin-2-one) to afford the proof-of-concept analogs **11**–**13** (Table 1). As the data in Table 1 demonstrate, all three

Table 1. Substituent effects on B-RAF activity

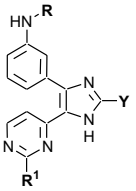

Compound	R	R^1	Y	B-RAF IC_{50} (μM)	V600E	C-RAF IC_{50} (μM)	RLM[a]	HLM[a]	pERk IC_{50} (μM)	Solubility[b] (μM)
11	CONHPh-3–CF_3-4–Cl	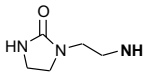	C_3H_5	0.066	0.022	0.014	44	50	2.3	6.2
12	CONHPh-3–CF_3-4–Cl	$NHCH_3$	C_3H_5	0.021	0.016	0.005	57	80	1.4	0.3
13	CONHPh-3–CF_3-4–Cl	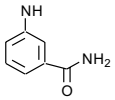	C_3H_5	0.035	0.061	0.031	nd	nd	2.1	0.4
14	SO_2CH_2Ph-3,4-Cl	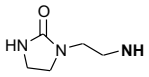	C_3H_5	0.343	0.141	0.041	52	85	na	na
15	SO_2CH_2Ph-3,4-Cl	$NHCH_3$	C_3H_5	0.469	0.138	0.026	87	60	na	na
16	SO_2CH_2Ph-3,4-Cl	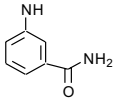	C_3H_5	0.887	0.274	0.049	44	76	na	na
17	$COCH_2$Ph-4-Cl	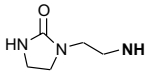	C_3H_5	0.007	0.002	0.001	60	38	3	35
18	$COCH_2$Ph-4-Cl	$NHCH_3$	C_3H_5	0.009	0.003	0.001	nd	nd	5.1	0.4
19	$COCH_2$Ph-4-Cl	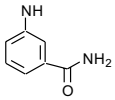	C_3H_5	0.004	0.003	0.0005	58	53	2.4	0.5
20	$COCH_2$Ph-4-Cl	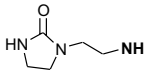	CF_3	0.054	0.04	0.02	34	73	30	7.5
21	$COCH_2$Ph-4-Cl	$NHCH_3$	CF_3	0.03	0.018	0.002	81	74	12.6	0.48
22	$COCH_2$Ph-4-Cl	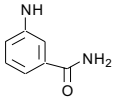	CF_3	0.108	0.085	0.017	47	71	30	0.35
3	BAY-43-9006/Sorafenib[c]			0.015	0.014	0.003	na	80	8.3	6.3

[a] Microsomal values are given as per cent of parent compound remaining after 30 min of incubation. The reported values are within a 10% range of error.

[b] Solubility was determined by the method reported in Ref. 9.

[c] Values were determined in-house.

analogs possessed good inhibitory activity against B-RAF kinase with IC_{50} values ranging from 21 to 66 nM, and slightly improved inhibition against the V600E mutant and C-RAF isoforms. Additionally, compounds **11**–**13** were slightly more potent than (**3**) at inhibiting ERK phosphorylation in a cellular assay. For example, compound **11**, which exhibited a better solubility profile by ~15-fold than the corresponding derivatives **12** and **13**, retained similar cellular activity. To improve compound solubility we replaced the urea moiety with similarly substituted sulfonamide and amide appendages. Table 1 shows that the sulfonamide analogs **14**–**16** displayed a 4- to 28-fold loss of kinase activity relative to ureas **11**–**13** , and lacked the necessary potency to be analyzed in the pERK cellular assay.[8] In contrast, the amide derivatives **17**–**19** provided a 2- to 10-fold increase in kinase potency relative to **11**–**13** ; however, a corresponding improvement in inhibiting ERK phosphorylation was not observed. Interestingly, while the solubility profile for compound **17** was enhanced 5-fold relative to compound **11**, this parameter did not translate to an increase in potency in the ERK phosphorylation cellular assay. One of the factors that appears to hamper the lack of correlation between enzyme potency and functional activity that we have observed in this series (Table 1) seems to be tied to the compounds solubility profile. Generally, it has been our observation that analogs exhibiting higher solubility

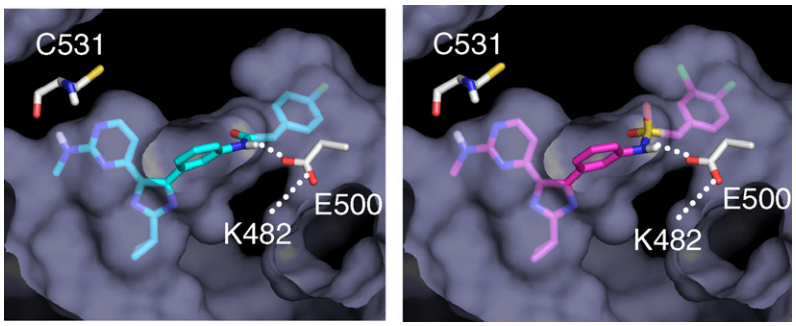

Figure 4. Docking models for the amide and sulfonamide analogs.

values displayed inferior functional activity. We attributed this to their difficulty in penetrating the lipophilic cellular membrane and hence, would be hindered from reaching the intracellular target.[9] Again, both the sulfonamide and amide derivatives displayed slightly better IC_{50} values against the V600E mutant and C-RAF isoforms than the wild-type isoform. It is worth noting that truncating the size of the substituent appended to the pyrimidine ring from the 1-(2-aminoethyl)-imidazolidin-2-one and 3-aminobenzamide moieties to the smaller methylamine group produced equivalent or better B-RAF kinase inhibition than the other two pyrimidine substituents.[10] This result was encouraging given that we were interested in reducing the molecular weight of the hybrid analogs. Moreover, modeling suggested that this group was directed to a solvent exposed region of the protein that was not expected to hinder the ATP pocket and allosteric binding interactions. Analogs containing the methylamine moiety also provided slightly improved rat and human microsomal stability data, although we observed a significant decrease in solubility relative to the 1-(2-aminoethyl)-imidazolidin-2-one moiety.

In an effort to correlate the observed B-RAF kinase inhibitory data to the interactions with the protein, we performed manual docking simulations using the data from the crystal structure.[2] The proposed binding mode for the amide moiety is shown in the left panel of Figure 4, in which the amide proton of the ligand forms a hydrogen bond with glutamic acid E500 of the kinase. The binding mode for the ureas is similar to the one shown here for the amides. Therefore, the difference in activity between the amides and the ureas (of up to 10-fold) may in part be due to a desolvation penalty that is incurred by the urea because of the presence of the extra nitrogen. Moreover, the glutamic acid E500 residue forms a salt bridge with the nearby lysine K482. From our modeling studies this suggests that E500 should not form two hydrogen bonds with the urea but rather only one, like the amide, with the proximal amide proton. In the right panel of Figure 4, the proposed binding mode for the sulfonamides shows that like the amides and the ureas the nitrogen atom makes a hydrogen bond interaction with E500. However, the most notable difference is the effect the 'extra' oxygen (shown by the arrow) has on the fit in the binding site. According to our docking models the sulfonamide analogs clash with the protein surface that leads to a binding destabilization relative to the amides or urea analogs. Hence, this additional conformational strain results in weaker B-RAF inhibitory activity.

Data from a related series of diarylimidazoles related to **1** and **2** demonstrated that replacing the cyclopropyl ring at the C2-position of the imidazole ring with a trifluoromethyl group tended to improve the solubility and metabolic stability for this class of compounds. These findings encouraged us to incorporate a trifluoromethyl group in this current hybrid-series as well. As the data in Table 1 illustrate relative to the amide analogs **17**–**19** , the trifluoromethyl derivatives **20**–**22** displayed a 3- to 26-fold decrease in kinase activity. Also, a measurable decrease in the potency of 2- to 12-fold was observed in the pERK cellular assay. Only the metabolic and solubility characteristics remained similar to those observed for the amide derivatives **17**–**19** . We postulate that the decrease in pERK cellular activity is due to the lower pK_a values associated with the C2-trifluoromethyl substituent, which causes the NH of the imidazole to become ionized under physiological pH.[11] Hence, the resulting charged species is less able to penetrate the lipid by-layer of the cell efficiently, and thus weaker functional activity is observed.

In summary, potent inhibitors of B-RAF kinase were identified that appear to bind to both the ATP binding pocket as well as an adjacent allosteric region. The current physiochemical and pharmacokinetic properties associated with these molecules, however, limit their evaluation in lengthy xenograph studies.[12] Compounds **11**, **14**, **17** and **20** were evaluated for kinase selectivity against a panel of 50 representative kinases (data not shown)[13] and only compounds **11** and **17** displayed >50% inhibition at 10 μM concentration against 4 kinases within the panel suggesting that identifying a selective B-RAF inhibitor is achievable.[14]

Acknowledgment

We express our thanks to Michele Rizzolio, Casey Lee and Michelle Herrmann for conducting the solubility and microsomal stability experiments for this study.

References and notes

1. (a) Davies, H.; Bignell, G. R.; Cox, C.; Stephens, P.; Edkins, S.; Clegg, S.; Teague, J.; Woffendin, H.; Garnett,

M. J.; Bottomley, W.; Davis, N.; Dicks, E.; Ewing, R.; Floyd, Y.; Gray, K.; Hall, S.; Hawes, R.; Hughes, J.; Kosmidou, V.; Menzies, A.; Mould, C.; Parker, A.; Stevens, C.; Watt, S.; Hooper, S.; Wilson, R.; Jayatilake, H.; Gusterson, B. A.; Cooper, C.; Shipley, J.; Hargrave, D.; Pritchard-Jones, K.; Maitland, N.; Chenevix-Trench, G.; Riggins, G. J.; Bigner, D. D.; Palmieri, G.; Cossu, A.; Flanagan, A.; Nicholson, A.; Ho, J. W. C.; Leung, S. Y.; Yuen, S. T.; Weber, B. L.; Seigler, H. F.; Darrow, T. L.; Paterson, H.; Marais, R.; Marshall, C. J.; Wooster, R.; Stratton, M. R.; Futreal, P. A. *Nature* **2002**, *417*, 949; (b) Bollag, G.; Freeman, S.; Lyons, J. F.; Post, L. E. *Curr. Opin. Invest. Drugs* **2003**, *4*, 1436.

2. Wan, P. T. C.; Garnett, M. J.; Roe, S. M.; Lee, S.; Niculescu-Duvaz, D.; Good, V. M.; Jones, C. M.; Marshall, C. J.; Springer, C. J.; Barford, D.; Marais, R. *Cell* **2004**, *116*, 855.
3. Pratilas, C. A.; Solit, D. B. *Rev. Recent Clin. trials* **2007**, *2*, 121, and references therein.
4. For example, human liver microsome stability values for the parent compounds **1** and **2** were 48% and 87% remaining after 15 min, respectively. The values for **1** and **2** in rat liver microsomes were 40% and 11%, respectively. Solubility values for **1** was 87 μM and for **2** was >100 μM at pH 7.4 (phosphate buffer).
5. Khire, U. R.; Bankston, D.; Barbosa, J.; Brittelli, D. R.; Caringal, Y.; Carlson, R.; Dumas, J.; Gane, T.; Heald, S. L.; Hibner, B.; Johnson, J. S.; Katz, M. E.; Kennure, N.; Kingery-Wood, J.; Lee, W.; Liu, X. G.; Lowinger, T. B.; McAlexander, I.; Monahan, M. K.; Natero, R.; Renick, J.; Riedl, B.; Rong, H.; Sibley, R. N.; Smith, R. A.; Wolanin, D. *Bioorg. Med. Chem. Lett.* **2004**, *14*, 783.
6. (a) Nahm, S.; Weinreb, S. M. *Tetrahedron Lett.* **1981**, *22*, 3815; (b) Maryanoff, B. E.; Kinny, W. A.; Lawson, E. C.; Luci, D. K.; Marchenko, N.; Sviridov, S. *International Patent Application Number*; WO2007/081995, pg 243 describes preparation of the N-Boc carbamate (**29b**) in place of the ethyl carbamate analog used to prepare **7** in Scheme 1.
7. Kornblum, N.; Powers, J. W.; Anderson, G. J.; Jones, W. J.; Larson, H. O.; Levand, O.; Weaver, W. M. *J. Am. Chem. Soc.* **1957**, *79*, 6562.
8. Compounds possessing IC_{50} values >100 nM in the B-RAF kinase assay did not meet the criteria for progression though the remaining portions of our assay paradigm.
9. The aqueous solubility of compounds was determined using the following method. First, compounds were diluted in DMSO to a concentration of 10 mM. Subsequently, these were diluted 1:100 in 1 mL of 70 mM NaH_2PO_4, pH 7.4, and mixed for 24 h at room temperature. The samples were then centrifuged at 14,000 rpm in a bench top microfuge (Model 5420, Eppendorf, Hamburg, Germany) for 15 min. After transferring 800 μL to a fresh tube, samples were re-centrifuged as above and 600 μL was then transferred to an HPLC vial. The samples were analyzed by reversed phase chromatography (Zorbax C_{18}, Agilent HPLC). Standards of 100, 10, and 1 μM were prepared in DMSO to generate a standard curve. Compound concentrations were determined by extrapolating peak areas from the standard curve generated from a linear regression analysis in Graph Pad Prism (GraphPad Software, San Diego, CA). The calculated Log *P* values for compounds **17**–**19** are 3.13, 4.20, and 5.07, respectively.
10. The main exception to this observation was the (NHMe) analog **15** which possessed a higher IC_{50} value than **14** by 1.4-fold. However, due to the substantially higher IC_{50} values for the sulfonamide analogs **14**–**16** , the (NHMe) substituent still ranks favorably for displaying excellent B-RAF kinase inhibition (Table 1).
11. pK_a calculations using Jaguar Software (Findlay, Illinois, 62534), showed that the trifluoromethyl analogs **20**–**22** have pK_a values of ~5.8 versus ~11.8 for the cyclopropyl analogs **17**–**19** .
12. Crawford, S.; Belajic, D.; Wei, J.; Riley, J. P.; Dunford, P. J.; Bembenek, S.; Fourie, A.; Edwards, J. P.; Karlsson, L.; Brunmark, A.; Wolin, R. L.; Blevitt, J. M. *Mol. Can. Ther.* **2008**, *7*, 492.
13. Upstate (Millipore) kinase panel. Millipore Corp. 290 Concord Rd. Billerica, MA 01821.
14. Takle, A. K.; Brown, M. J. B.; Davies, S.; Dean, D. K.; Francis, G.; Gaiba, A.; Hird, A. W.; King, F. D.; Lovell, P. J.; Naylor, A.; Reith, A. D.; Steadman, J. G.; Wilson, D. M. *Bioorg. Med. Chem. Lett.* **2006**, *16*, 378.